

Enhancing One-Dimensional Charge Transport through Intermolecular π -Electron Delocalization: Conductivity Improvement for Organic Nanobelts

Yanke Che,[†] Aniket Datar,[†] Xiaomei Yang,[†] Tammene Naddo,[†] Jincui Zhao,^{*,‡} and Ling Zang^{*,†}

Department of Chemistry and Biochemistry, Southern Illinois University, Carbondale, Illinois 62901, and Key Laboratory of Photochemistry, Institute of Chemistry, Chinese Academy of Sciences, Beijing 100080, China

Received January 9, 2007; E-mail: lzang@chem.siu.edu; jczhao@iccas.ac.cn

Electrical conductivity of organic semiconductor materials represents one of the critical parameters that control the performance efficiency of organic-based electronic and optoelectronic devices. For materials assembled from planar aromatic molecules, evidence suggests that charge carrier mobility is usually maximized along the direction of cofacial π - π stacking of the molecules.^{1–3} While such conductivity optimization can be realized in the single crystalline phase, it is usually challenging to prepare a single crystal at large scale, and moreover it is difficult to unveil the orientation of molecular stacking within a bulk crystal when aligning it in a device, where directional control of charge transport is often demanded. To this end, fabrication of one-dimensional nanomaterials (e.g., nanowires) with cofacial molecular stacking along the long-axis of nanowire becomes essential in both fundamental investigation and practical application development. Such nanowires enable investigations that may lead to direct correlation between the maximized conductivity and the optimized molecular stacking.²

Recently, great progress has been made in fabricating nanowires or nanobelts from large, rigid, conjugate molecules, for which the molecular π - π stacking is mostly along the long-axis of nanowire (or nanobelt).^{3,4} While theoretical modeling and calculation suggest efficient intermolecular π -electron delocalization (and thus enhanced conductivity) along the molecular stacking,^{5,6} there are few studies reported on the experimental characterization and evaluation of such π -electron delocalization and the effect on electrical conductivity.^{7,8} In this Communication, we report a direct probing of the delocalized charge within a PTCDI nanobelt (a special nanowire with beltlike morphology) using ESR spectrometry methods. The efficient π -electron delocalization is consistent with the high conductivity measured with the same nanobelt.

The PTCDI molecule employed (shown in Scheme 1) has proven effective for cofacial π - π stacking owing to the minimal side-chain steric hindrance.^{9,10} Highly uniform nanobelts can be fabricated from this molecule using phase-transfer self-assembly that was previously developed in our lab.¹¹ Compared to common nanowires with round cross section, a nanobelt will provide large area interface when deposited on electrodes, thus facilitating the fabrication of devices with improved electrical contact.

When reacting with a strong reducing reagent (e.g., hydrazine, $E^{\circ}_{\text{ox}} = +0.43$ V, vs SCE), PTCDI ($E^{\circ}_{\text{red}} = -0.59$ V, vs SCE¹²) was reduced to an anionic radical (Figure 1), which is stable in an oxygen free environment. The spectral structure of the radical obtained matches the standard spectra of PTCDI radicals that were obtained by reacting with metal sodium.^{12,13} Under argon protection, the radical sustained for extended time (inset of Figure 1). More importantly, the transformation between the neutral and radical state of PTCDI is reversible, that is, the neutral PTCDI can be recovered from the radical simply by removing the hydrazine via solvent

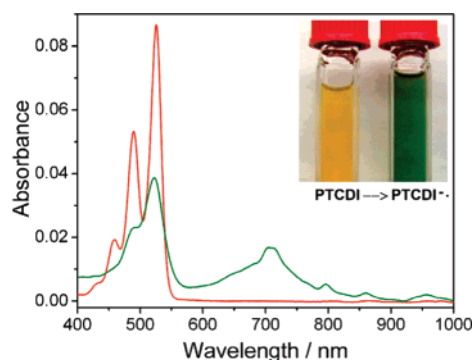
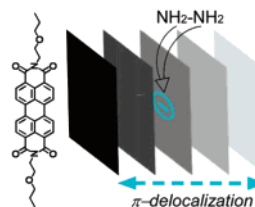


Figure 1. UV-vis absorption spectra showing the conversion of PTCDI molecule (1.0 μM in DMF, red line) into anionic radical (green) in the presence of hydrazine (0.1 M). The inset shows the dramatic color change indicative of radical formation in DMF.

Scheme 1. Enhancing One-Dimensional Electrical Conductivity through Cofacial π -Electronic Delocalization of Doped Charges



extraction. The high stability observed for the PTCDI radical is likely due to the efficient in-plane delocalization of the charge over the whole PTCDI skeleton. Such in-plane electron delocalization is consistent with the typical n-type character of PTCDI materials as evidenced in real devices.¹⁴ The stable charged state makes PTCDI an ideal candidate for investigating the cofacial π -electron delocalization, mimicking the vertical (interplanar) charge migration within graphite.

The stable anionic radical was also measured by electron spin resonance (ESR) spectrometry, with which a hyperfine spectrum of the radical was observed (Figure S2), consistent with previous observation by others.¹³ When cofacially stacked into a columnar phase within a nanobelt, the PTCDI anionic radical loses the hyperfine structure in ESR spectrum. Furthermore, in contrast to the symmetric spectrum (with g -tensor of 2.0033) observed for the free radical (Figure 2), the ESR spectrum of the anionic-doped nanobelt loses the reflection symmetry about the line center, showing an anisotropic g -tensor, with g (2.0038) $>$ g (2.0026). Similar asymmetric ESR spectrum was obtained for PTCDI stacking in films.¹³ The anisotropic g -tensor is consistent with the uniaxial property of the nanobelt, which is dominated by the cofacial stacking of PTCDI.^{9,10} This observation, along with the lack of hyperfine ESR spectrum, implies strong intermolecular π -electron delocalization along the long axis of nanobelt.

[†] Southern Illinois University.
[‡] Chinese Academy of Sciences.

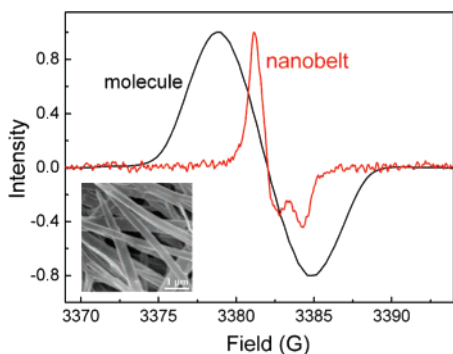


Figure 2. Comparison of ESR spectra of free anionic radicals dissolved in DMF (25 μM) and the negatively charged nanobelt dispersed in methanol (1 mM). The inset shows the SEM image of PE-PTCDI nanobelts, width ca. 500 nm and thickness ca. 100 nm.

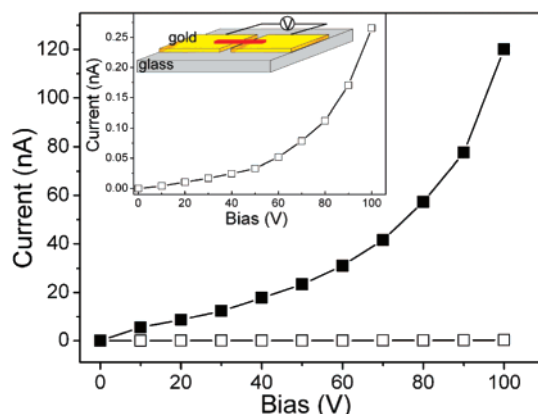


Figure 3. I–V curves measured on a PTCDI nanobelt: (□) in air; (■) in saturated hydrazine vapor. The inset is an enlarged plot of the I–V curve in air, and schematic illustration of the two-electrode device fabricated on glass with a single nanobelt deposited across atop the gap (80 μm).

As a control, nanoparticles formed from a PTCDI molecule with bulky, branched side chains were employed for the same ESR investigations (Figure S3). It was previously evidenced that because of the strong side-chain steric hindrance, no effective cofacial π – π stacking is allowed for the aggregate of this molecule.¹¹ Consistently, the observed ESR spectrum of the reduced nanoparticles shows similar structure as the free anionic radical, supporting the conclusion that the asymmetric ESR spectrum observed for the nanobelt is predominantly due to the cofacial π -electron delocalization along the long-axis.

Considering the efficient charge separation between hydrazine and PTCDI, and the high stability of the anionic radical thus produced, the conductivity of PTCDI nanobelts can feasibly be enhanced through surface n-type doping with hydrazine, for example, immersing the nanobelts in a saturated vapor of hydrazine. Under an applied bias, the doped electrons will rapidly migrate along the long axis of the nanobelt (owing to the long-range π -electron delocalization between the cofacially stacked PTCDI molecules), leading to significant enhancement in current. Figure 3 shows the current–voltage (I–V) measurement performed on a single nanobelt fabricated from the PTCDI molecule shown in Scheme 1 (see Supporting Information for device fabrication). As previously observed for conducting polymer nanowires,¹⁵ the I–V curve measured with the PTCDI nanobelt becomes nonlinear at higher bias, implying an injection-limited charge transport.¹⁶ For four devices measured, the conductivity extracted from the quasi-

linear region at low bias (up to 50 V) is ca. $1.0 \times 10^{-3} \text{ S m}^{-1}$, a value about 1 order of magnitude higher than that measured from polymer nanowires (e.g., polythiophene).^{15a} The high conductivity observed is consistent with the ordered one-dimensional π – π stacking (cofacial π -electron delocalization) as evidenced above by ESR.

Upon saturated with hydrazine vapor, the current was dramatically increased by about 3 orders of magnitude, mainly because of the electron donation from hydrazine through electron-donor–electron-acceptor complexation with PTCDI. Such a charge separation process is facilitated coincidentally by the intramolecular π -electron delocalization within the PTCDI skeleton and the intermolecular π -electron delocalization along the long-axis of nanobelt. The maximal conductivity obtained with saturated hydrazine vapor was estimated in the range of 0.5–1.0 S m^{-1} , more than 2 orders of magnitude higher than that of undoped silicon ($1.6 \times 10^{-3} \text{ S m}^{-1}$).¹⁷

In summary, effective π -electron delocalization within a PTCDI nanobelt has been experimentally characterized by ESR and I–V measurements. The long-range π -electron delocalization enables enhancement of electrical conductivity of the nanobelt through surface doping. More systematic investigation will be made on sensor development of the nanobelt for various reducing gaseous species, including organic amines, CO, and NO.

Acknowledgment. This work was supported by NSF (Grant CMMI 0638571) and NSFC (Grant No. 20520120221).

Supporting Information Available: Sample preparation; device fabrication; spectral, ESR, I–V measurements. This material is available free of charge via the Internet at <http://pubs.acs.org>.

References

- Guillon, D. *Struct. Bonding (Berlin)* **1999**, *95*, 41–82.
- Hoeben, F. J. M.; Jonkheijm, P.; Meijer, E. W.; Schenning, A. P. H. J. *Chem. Rev.* **2005**, *105*, 1491–1546.
- Grimdale, A. C.; Mullen, K. *Angew. Chem., Int. Ed.* **2005**, *44*, 5592.
- Samori, P.; Francke, V.; Mullen, K.; Rabe, J. P. *Chem.–Eur. J.* **1999**, *5*, 2312–2317.
- Lemaire, V.; da Silva Filho, D. A.; Coropceanu, V.; Lehmann, M.; Geerts, Y.; Piris, J.; Debije, M. G.; van de Craats, A. M.; Senthilkumar, K.; Siebbeles, L. D. A.; Warman, J. M.; Bredas, J.-L.; Cornil, J. *J. Am. Chem. Soc.* **2004**, *126*, 3271–3279.
- Rochefort, A.; Martel, R.; Avouris, P. *Nano Lett.* **2002**, *2*, 877–880.
- Jackel, F.; Watson, M. D.; Mullen, K.; Rabe, J. P. *Phys. Rev. B* **2006**, *73*, 045421–045426.
- Crispin, X.; Cornil, J.; Friedlein, R.; Okudaira, K. K.; Lemaire, V.; Crispin, A.; Kestemont, G.; Lehmann, M.; Fahlman, M.; Lazzaroni, R.; Geerts, Y.; Wendin, G.; Ueno, N.; Bredas, J.-L.; Salaneck, W. R. *J. Am. Chem. Soc.* **2004**, *126*, 11889–11899.
- Balakrishnan, K.; Datar, A.; Oitker, R.; Chen, H.; Zuo, J.; Zang, L. *J. Am. Chem. Soc.* **2005**, *127*, 10496–10497.
- Datar, A.; Balakrishnan, K.; Yang, X. M.; Zuo, X.; Huang, J. L.; Yen, M.; Zhao, J.; Tiede, D. M.; Zang, L. *J. Phys. Chem.* **2006**, *110*, 12327–12332.
- Balakrishnan, K.; Datar, A.; Naddo, T.; Huang, J.; Oitker, R.; Yen, M.; Zhao, J.; Zang, L. *J. Am. Chem. Soc.* **2006**, *128*, 7390–7398.
- Kircher, T.; Lohmannsroben, H.-G. *Phys. Chem. Chem. Phys.* **1999**, *1*, 3987–3992.
- Chen, S.-G.; Branz, H. M.; Eaton, S. S.; Taylor, P. C.; Cormier, R. A.; Gregg, B. A. *J. Phys. Chem. B* **2004**, *108*, 17329–17336.
- Newman, C. R.; Frisbie, C. D.; da Silva Filho, D. A.; Bredas, J.-L.; Ewbank, P. C.; Mann, K. R. *Chem. Mater.* **2004**, *16*, 4436–4451.
- (a) O'Brien, G. A.; Quinn, A. J.; Tanner, D. A.; Redmond, G. *Adv. Mater.* **2006**, *18*, 2379. (b) Aleshin, A. N.; Lee, H. J.; Park, Y. W.; Akagi, K. *Phys. Rev. Lett.* **2004**, *93*, 196601. (c) Lee, H. J.; Jin, Z. X.; Aleshin, A. N.; Lee, J. Y.; Goh, M. J.; Akagi, K.; Kim, Y. S.; Kim, D. W.; Park, Y. W. *J. Am. Chem. Soc.* **2004**, *126*, 16722.
- Stutzmann, N.; Friend, R. H.; Siringhaus, H. *Science* **2003**, *299*, 1881–1884.
- Serway, R. A. *Principles of Physics*, 2nd ed; Saunders College: Fort Worth, TX; London, 1998; p 602.

JA070164G